Molecular Microbiology (2010) 75(4), 1021–1032 ■
doi:10.1111/j.1365-2958.2009.07039.x
First published online 15 January 2010

Membrane fluidity determines sensitivity of filamentous fungi to chitosan

J. Palma-Guerrero,[1]* J. A. Lopez-Jimenez,[2] A. J. Pérez-Berná,[3] I.-C. Huang,[4] H.-B. Jansson,[1] J. Salinas,[1] J. Villalaín,[3] N. D. Read[4] and L. V. Lopez-Llorca[1]

[1]*Laboratory of Plant Pathology, Multidisciplinary Institute for Environmental Studies (MIES) Ramón Margalef, Department of Marine Sciences and Applied Biology, University of Alicante, E-03080 Alicante, Spain.*
[2]*Physiology Department, Faculty of Biology, University of Murcia, E-30100 Murcia, Spain.*
[3]*Instituto de Biología Molecular y Celular, Universidad Miguel Hernández, E-03202 Elche-Alicante, Spain.*
[4]*Fungal Cell Biology Group, Institute of Cell Biology, University of Edinburgh, Rutherford Building, Edinburgh EH9 3JH, UK.*

Summary

The antifungal mode of action of chitosan has been studied for the last 30 years, but is still little understood. We have found that the plasma membrane forms a barrier to chitosan in chitosan-resistant but not chitosan-sensitive fungi. The plasma membranes of chitosan-sensitive fungi were shown to have more polyunsaturated fatty acids than chitosan-resistant fungi, suggesting that their permeabilization by chitosan may be dependent on membrane fluidity. A fatty acid desaturase mutant of *Neurospora crassa* with reduced plasma membrane fluidity exhibited increased resistance to chitosan. Steady-state fluorescence anisotropy measurements on artificial membranes showed that chitosan binds to negatively charged phospholipids that alter plasma membrane fluidity and induces membrane permeabilization, which was greatest in membranes containing more polyunsaturated lipids. Phylogenetic analysis of fungi with known sensitivity to chitosan suggests that chitosan resistance may have evolved in nematophagous and entomopathogenic fungi, which naturally encounter chitosan during infection of arthropods and nematodes. Our findings provide a method to predict the sensitivity of a fungus to chitosan based on its plasma membrane composition, and suggests a new strategy for antifungal therapy, which involves treatments that increase plasma membrane fluidity to make fungi more sensitive to fungicides such as chitosan.

Accepted 21 December, 2009. *For correspondence. E-mail jpalma@ua.es; Tel. (+34) 965903400 ext 2223; Fax (+34) 965909897.

Introduction

Chitosan is a partly deacetylated form of chitin, the β-(1,4)-D-linked polymer of N-acetylglucosamine. Chitin is a natural polymer which is only second in abundance to cellulose (Kumar, 2000), and is a common constituent of arthropod exoskeletons, nematode eggshells, most fungal cell walls, some algal cell walls, and some protozoan cysts (Cohen, 1987). Chitosan has a pK_a value of ~6.3 and thus it is cationic at lower pH values due to protonation of its amino groups. Chitosan's positive charge confers it with biological properties that give it great potential in medicine and agriculture (Kumar, 2000). Chitosan is non-toxic to mammals and higher animals (Dodane and Vilivalam, 1998) and elicits plant defence mechanisms (Benhamou *et al.*, 1994; Trotel-aziz *et al.*, 2006). Other positively charged polymers, such as poly-L-lysine, protamine and histones (Hadwiger *et al.*, 1977), and many cationic peptides from insects, humans and plants (Selitrennikoff, 2001), also have antifungal properties. Chitosan has the advantage over cationic antifungal peptides that chitin provides an unlimited natural source for chitosan production, and peptides are susceptible to protease digestion. Most commercial chitosan is obtained by chemical deacetylation of crustacean chitin from shellfish waste (Kumar, 2000).

Since Allan and Hadwiger in 1979 (Allan and Hadwiger, 1979) first showed the fungicidal effect of chitosan it has attracted much research, and several studies have attempted to elucidate its mode of action (Rabea *et al.*, 2003). The inhibitory activity of chitosan against phytopathogenic fungi depends on it having a low molecular weight, high degree of deacetylation and being under acidic conditions for its amino groups to be charged (Stössel and Leuba, 1984). Chitosan also exhibits antibiotic activity against bacteria and yeasts, and has been reported to damage their plasma membranes (Helander *et al.*, 2001; Liu *et al.*, 2004; Zakrzewska *et al.*, 2005). The fungicidal effects of chitosan on filamentous fungi have recently been shown to involve energy-dependent plasma

Fig. 1. Uptake of rhodamine-chitosan by chitosan-sensitive fungi (*Neurospora crassa*, *Fusarium oxysporum* f.sp. *radicis-lycopersici*), but not chitosan-resistant fungi (*Pochonia chlamydosporia*, *Beauveria bassiana*). Bar = 2 μm.

membrane permeabilization (Palma-Guerrero *et al.*, 2009).

We recently showed that most plant pathogenic fungi are chitosan-sensitive, whereas nematophagous and entomopathogenic fungi are chitosan-resistant (Palma-Guerrero *et al.*, 2008). In the present study we have analysed the basis of this sensitivity and resistance to chitosan. We have characterized plasma membrane components of both chitosan-resistant and chitosan-sensitive fungi and determined the lipid components of the plasma membrane that confer chitosan sensitivity. Based on these data, we propose a model for chitosan-induced membrane permeabilization and suggest an evolutionary explanation for chitosan resistance in nematophagous and entomopathogenic fungi. Our results also suggest a new strategy for the design of antifungal agents.

Results

The plasma membrane forms a barrier to chitosan in chitosan-resistant fungi

Rhodamine-labelled chitosan (R-chitosan) has been previously shown to enter the spores (conidia) of the chitosan-sensitive fungi after causing plasma membrane permeabilization (Palma-Guerrero *et al.*, 2009). We compared R-chitosan uptake by conidia of chitosan-sensitive and chitosan-resistant fungi. Chitosan-sensitive species used were the saprotroph *N. crassa* and the plant pathogen *Fusarium oxysporum* f. sp. *radicis-lycopersici*; the nematophagous fungus *Pochonia chlamydosporia* and the entomopathogenic fungus *Beauveria bassiana* were selected for being chitosan-resistant (Palma-Guerrero *et al.*, 2008; 2009). Fifteen minutes after application, R-chitosan fluorescence was detected both on the surface and within all conidia of the two chitosan-sensitive species (Fig. 1) as shown previously (Palma-Guerrero *et al.*, 2008; 2009). In the chitosan-resistant fungi *P. chlamydosporia* and *B. bassiana*, however, R-chitosan fluorescence was only detected on the conidial surface (Fig. 1) and less than 30% of these conidia showed intracellular R-chitosan fluorescence.

Plasma membrane composition of chitosan-sensitive fungi exhibit increased fluidity

To assess the importance of fungal plasma membrane composition on chitosan sensitivity, we analysed the main fatty acids, ergosterol, phospholipids and acidic glycosphingolipids in chitosan-sensitive and resistant-fungi. Fatty acid analyses revealed that both chitosan-sensitive fungi have significantly higher levels of the polyunsaturated fatty acid linolenic acid (C18:3 ω-3), but lower levels of saturated palmitic (C16:0) and stearic (C18:0) acids and the mono-unsaturated oleic acid (C18:1 ω-9) than the two chitosan-resistant fungi (Table 1). The linoleic acid content was similar in both types of fungi. The fatty acid unsaturation indexes (Thompson *et al.*, 1992) of *N. crassa* and *F. oxysporum* were 148 ± 0.7 and 157 ± 1.7 respectively, which were significantly higher than those of the resistant *P. chlamydosporia* (121 ± 7.9) and *B. bassiana* (111 ± 5.1). Phospholipid head groups have previously been proposed as the possible target for chitosan binding (El Ghaouth and Arul, 1992). In this way, the different chitosan sensitivities of different fungi have been speculated to be due to differences in phospholipid composition, and particularly the nature of the charged phospholipid heads (Laflamme *et al.*, 1999). We found no correlation between phospholipid composition and chitosan sensitivity; similar relative amounts of the negatively charged phospholipids were found in all four species (Table 2). The phospholipids from chitosan-sensitive fungi, however, had increased amounts of polyunsaturated fatty acids (Table 3), confirming the results obtained in the fatty acid analysis. Ergosterol is an important component of fungal plasma membranes, contributing to their rigidity, stability and resistance to physical stresses (Parks and Casey, 1995). The ergosterol content of the four species varied, but no correlation was found with chitosan sensitivity (Fig. 2A). GIPCs are acidic glycosphingolipids

Table 1. Fatty acid (FA) composition (% fatty acid ± SD) of chitosan-sensitive and -resistant fungi, and an FA desaturase mutant (Δ*ods*) of *N. crassa*.

	Chitosan-sensitive		Chitosan-resistant		FA desaturase mutant
FA	*N. crassa*	*F. oxysporum*	*P. chlamydosporia*	*B. bassiana*	*N. crassa* Δ*ods*
Palmitic acid (C16:0)	18.45 ± 0.19^a	14.85 ± 0.32^b	21.36 ± 2.17^c	23.40 ± 1.30^c	11.91 ± 0.23^b
Stearic acid (C18:0)	3.52 ± 0.03^a	5.39 ± 0.77^b	7.14 ± 1.33^c	9.69 ± 0.97^d	0.83 ± 1.43^a
Oleic acid (C18:1 ω-9)	12.15 ± 0.37^a	13.79 ± 1.0^a	19.47 ± 0.40^b	19.99 ± 0.14^b	81.63 ± 0.64^b
Linoleic acid (C18:2 ω-6)	47.29 ± 0.20^a	43.98 ± 1.16^b	48.64 ± 3.04^c	39.46 ± 2.49^d	0.16 ± 0.08^b
Linolenic acid (C18:3 ω-3)	10.58 ± 0.22^a	16.77 ± 0.96^b	0.03 ± 0.01^c	3.23 ± 0.33^d	0.55 ± 0.01^b

The plasma membrane of chitosan-sensitive fungi possess more polyunsaturated fatty acids than do chitosan-resistant fungi. Different superscript letters indicate significant differences ($P < 0.05$) between fungi for each FA. Each value represents the mean of three replicates.

that contain ionizable functional groups and are localized in the plasma membranes of fungi, plants and protozoa, but have not been found in cells or tissues of mammals or other higher animals (Patton and Lester, 1991). In fungi they constitute 20–30% of total lipids, and have been previously proposed as a possible target for chitosan binding (Zakrzewska *et al.*, 2005). Again, no clear correlation between GIPC profiles and differences in chitosan sensitivity between fungi could be established (Fig. 2B).

Chitosan sensitivity can be modified by altering plasma membrane fluidity

A deletion mutant of an *N. crassa* fatty acid desaturase was used to test whether depleting the plasma membrane of polyunsaturated fatty acids increased its resistance to chitosan. The gene encoding this *N. crassa* enzyme is an orthologue of the *A. nidulans* gene (An2) encoding oleoyl-Δ12 desaturase, which generates linoleic acid (C18:2) from oleic acid (C18:1) (Damude *et al.*, 2006). The fatty acid profiles of the knockout mutant of the *N. crassa* oleoyl-Δ12 desaturase gene (NCU02209.3), which we have named *ods*, confirmed that it had been deleted. Both linoleic and linolenic acid were virtually absent from this mutant, confirming that linoleic acid is not produced in the absence of the enzyme, and oleic acid accumulated (Table 1). The fatty acid unsaturation index for the Δ*ods* mutant was 89 ± 1.2 compared with 148 ± 0.7 for the wild-type.

Mycelial growth of the Δ*ods* mutant was significantly less sensitive to 1 mg ml^{-1} chitosan than that of the wild-type (Fig. 3). To assess the inhibitory effects of chitosan on conidial germination and conidial anastomosis tubes (CATs) fusion (Roca *et al.*, 2005) during colony establishment, the chitosan concentration was reduced to 0.6 μg ml^{-1}, because these processes are particularly chitosan sensitive (Palma-Guerrero *et al.*, 2008; 2009). The *Δods* mutant showed significantly reduced inhibition of conidial germination and CAT fusion by chitosan compared with the wild-type (Fig. 3).

Chitosan-induced leakage was greatest across artificial membranes composed of unsaturated phospholipids

In order to assess the effect of chitosan on membrane destabilization, we studied its effect on the release of the fluorescent probe, calcein, encapsulated in artificial liposomes of different membrane compositions (Fig. 4A). Chitosan induced the release of dye from the liposomes in a dose-dependent manner. The greatest leakage was from liposomes containing the negatively charged phospholipids phosphatidylglycerol (PG) or 1,2-dimyristoyl-sn-

Table 2. Phospholipid composition (mg phospholipids g^{-1} dried mycelium) of chitosan-sensitive and -resistant fungi.

		Chitosan-sensitive		Chitosan-resistant	
	Phospholipid	*N. crassa*	*F. oxysporum*	*P. chlamydosporia*	*B. bassiana*
Anionic	Phosphatidylglycerol	0.24	1.92	0.43	0.2
	Phosphatidylserine	1.33	1.65	1.46	2.28
	Phosphatidic acid	0.89	1.35	1.33	0.65
	Diphosphatidylglycerol	1.05	1.65	1.62	1.1
	Phosphatidylinositol	1.23	2.11	1.91	1.56
Neutral lipids	Phosphatidylethanolamine	3.62	6.15	4.54	5.03
	Phosphatidylcholine	8.52	7.05	9.09	9.86
	Lysophosphatidylcholine	0.31	0.56	0.84	0.37

No correlation with chitosan sensitivity was found.

Table 3. Phospholipid fatty acid composition (% total fatty acid content) of chitosan-sensitive and chitosan-resistant fungi.

			Anionic phospholipids					Neutral phospholipids		
	Fungus	Fatty acid	PG	PS	PA	DPG	PI	PE	PC	LysoPC
Chitosan-sensitive	*N. crassa*	16:0	32.70	43.76	31.55	21.20	43.47	27.89	8.71	29.07
		18:0	38.90	2.42	13.27	16.38	3.83	2.78	2.70	37.14
		18:1 (ω-9)	10.03	10.08	9.66	11.65	8.81	10.03	14.37	12.03
		18:2 (ω-6)	9.39	37.73	36.04	38.80	36.50	50.75	60.60	8.20
		18:3 (ω-3)	1.27	3.56	4.18	5.72	3.52	4.96	8.91	0.00
	F. oxysporum	16:0	40.35	41.75	24.76	11.69	39.55	20.75	7.33	28.88
		18:0	12.71	5.77	11.70	15.47	9.74	6.36	7.97	46.08
		18:1 (ω-9)	13.66	11.59	14.28	10.23	9.13	16.21	13.59	8.14
		18:2 (ω-6)	21.17	30.80	33.84	38.18	27.51	43.07	47.07	4.26
		18:3 (ω-3)	5.60	8.26	11.30	20.73	8.63	10.79	20.93	0.65
	P. chlamydosporia	16:0	34.71	45.30	26.34	21.41	45.05	25.82	7.55	30.77
		18:0	31.74	4.22	13.63	20.39	5.59	4.17	3.00	44.18
		18:1 (ω-9)	10.04	9.41	10.99	8.17	7.52	14.14	8.72	9.26
		18:2 (ω-6)	9.83	40.43	46.12	46.34	40.04	54.87	79.53	4.07
		18:3 (ω-3)	0.00	0.00	0.00	0.00	0.00	0.00	0.00	0.00
Chitosan-resistant	*B. bassiana*	16:0	28.03	44.38	32.23	18.20	43.88	23.75	6.96	32.01
		18:0	40.95	5.56	35.16	21.79	10.83	5.93	4.02	30.66
		18:1 (ω-9)	8.56	18.82	12.59	13.92	13.37	25.94	23.67	13.87
		18:2 (ω-6)	4.00	29.88	15.11	41.52	29.80	42.08	61.80	8.36
		18:3 (ω-3)	0.00	0.43	0.67	1.20	0.38	0.98	1.60	0.00

The phospholipids of chitosan-sensitive fungi had increased amounts of polyunsaturated fatty acids. No correlation between the type of phospholipid present and chitosan sensitivity was found in the different fungi.
DPG, diphosphatidylglycerol; LysoPC, lysophospatidylcholine; PA, phosphatidic acid; PC, phosphatidylcholine; PE, phosphatidylethanolamine; PG, phosphatidylglycerol; PI, phosphatidylinositol; PS, phosphatidylserine.

glycero-3-[phospho-rac-(1-glycerol)] (DMPG). Leakage from liposomes composed of the neutral phospholipids phosphatidylcholine (PC) or 1,2-dimyristoyl-sn-glycero-3-phosphocholine (DMPC) was significantly lower. We also assayed the effect of chitosan on membranes containing different ergosterol concentrations and observed that ergosterol decreased chitosan-induced leakage (Fig. 4A) possibly due to an increase in membrane stability. Unsaturated fatty acids in neutral membranes containing 18:3(*cis*)phosphatidylcholine significantly increased the leakage, whereas for negatively charged membranes containing 18:3(*cis*)phosphatidylglycerol the leakage increase was much lower.

The effect of chitosan on the structural and temperature-dependent properties of phospholipid membranes was investigated by measuring the steady-state fluorescence anisotropy of the fluorescent probes diphenyl-1,3,5-hexatriene (DPH) and 1-(4-trimethylammoniumphenyl)-6-phenyl-1,3,5-hexatriene (TMA-DPH) incorporated into artificial membranes composed of either negatively charged DMPG or neutral DMPC (Fig. 4B–E). These saturated, synthetic phospholipids were used because they have optimal properties for analysing temperature-dependent phospholipid anisotropy and structural order in membranes when used in combination with DPH and TMA-DPH (Lentz, 1993). The location of these fluorescent probes in the membrane differs: TMA-DPH localizes close to the water/lipid interface and its fluorophore is located in the upper part of the acyl chain region, while DPH (lacking a polar group) is embedded deeper in the hydrophobic part of the bilayer (Mateo *et al.*, 1991). The influence of chitosan on DMPC and DMPG vesicles was assessed at different temperatures (Fig. 4B–E). Chitosan did not have a significant effect on the main phospholipid transition in DMPC membranes (Fig. 4D and E), although a slight increase in anisotropy values in the gel phase and a decrease in the liquid-crystalline phase for the TMA-DPH probe were found (Fig. 4E). However, in the case of the negative phospholipid DMPG, the presence of chitosan dramatically affected the cooperativity and the anisotropy of the gel and liquid-crystalline phases of DMPG, increasing the anisotropy values in the liquid-crystalline phase and decreasing them in the gel phase (Fig. 4B and C). This effect was more significant for TMA-DPH than DPH. These results suggest that chitosan is located close to the TMA-DPH along the membrane surface, decreasing the cooperativity of the main phospholipids transition and changing the anisotropy values to a point where a gel-to-liquid-crystalline phase transition can hardly be detected.

Discussion

In this study we have investigated the mode-of-action of the antifungal agent chitosan, a topic that has been studied for more than 30 years but was little understood until now. Our multidisciplinary approach, combining cell

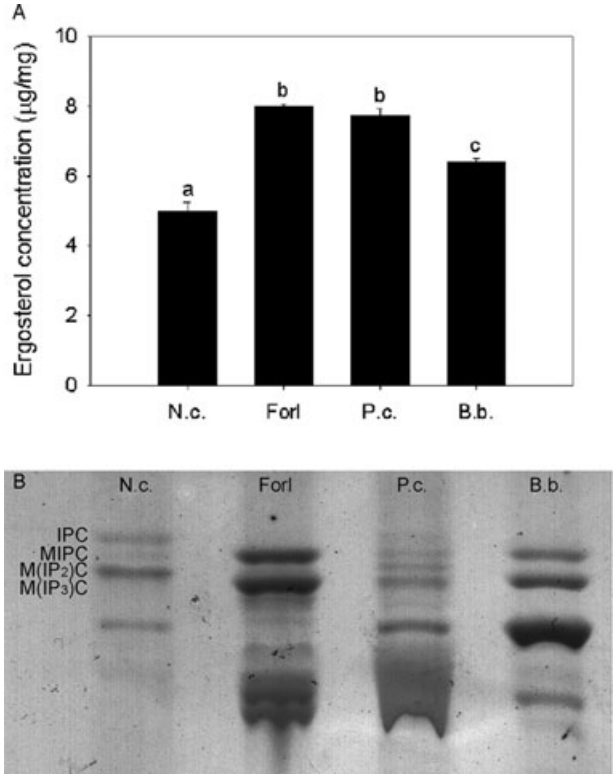

Fig. 2. Ergosterol and glycosphingolipids (GIPCs) content of chitosan-sensitive and chitosan-resistant fungi.
A. Ergosterol content (±SE). Letters show statistical differences between fungi. Values with different letters are significantly different ($P < 0.05$). Each value represents the mean of three replicates.
B. HPTLC profiles of GIPCs. Labels on the left show relative migrations in solvent F of inositol-, mannosylinositol-, mannosyldiinositol- and mannosyltriinositolphosphorylceramide [IPC, MIPC, M(IP_2)C and M(IP_3)C respectively] according to references (Bennion *et al.*, 2003; Ferket *et al.*, 2003). B.b., *Beauveria bassiana* (chitosan resistant); Forl, *Fusarium oxysporum* f.sp. *radicis-lycopersici* (chitosan sensitive); N.c., *Neurospora crassa* (chitosan sensitive); P.c., *Pochonia chlamydosporia* (chitosan resistant).

biology, biochemical, genetic and biophysics techniques, has demonstrated that the antifungal activity of chitosan depends on the fluidity of the fungal plasma membrane, which is determined by its polyunsaturated fatty acid composition.

By imaging fluorescently labelled chitosan using confocal microscopy we have shown that chitosan binds to the conidial surfaces of all species tested, but only consistently permeabilizes the plasma membranes of chitosan-sensitive fungi. This suggests that the plasma membrane forms a barrier to chitosan in chitosan-resistant fungi. The analysis of the main plasma membrane components revealed important differences in fatty acid composition between chitosan-sensitive and chitosan-resistant fungi. A higher content of the polyunsaturated fatty acid linolenic acid and a higher unsaturation index was measured in the membranes of chitosan-sensitive fungi. This indicates that the plasma membranes of chitosan-sensitive fungi have a higher fluidity than those of chitosan-resistant ones. No correlation between chitosan sensitivity and phospholipid, ergosterol or GIPC composition was found.

The importance of fatty acid composition on chitosan sensitivity was confirmed using an *N. crassa* Δ*ods* mutant, which lacks the enzyme oleoyl-Δ12 desaturase and possesses membranes without linoleic and linolenic acid. The Δ*ods* mutant showed increased resistance to chitosan in terms of mycelial growth, conidial germination and CAT fusion. This finding further supports the conclusion that the polyunsaturated fatty acid composition of the plasma membrane, and thus membrane fluidity, is important for conferring chitosan sensitivity. These results confirm the result observed by Zakrzewska *et al.* (2007) in the yeast *S. cerevisiae*, who observed that treatments that increase plasma membrane fluidity, such as increased growth temperature or ergosterol synthesis inhibition by miconazole, sensitize *S. cerevisiae* to chitosan (Zakrzewska *et al.*, 2007). We found no changes in chitosan sensitivity in *N. crassa* grown at different temperatures (unpublished results). This is perhaps not surprising because *N. crassa* has previously been shown to be able to maintain its membrane fluidity constant by modifying its membrane fatty acid composition at different temperatures (Vokt and Brody, 1985).

Experiments with artificial membranes indicated that membrane disruption involves electrostatic interactions between positively charged chitosan and the negative phospholipid headgroups, as has been previously suggested (El Ghaouth and Arul, 1992). We found that leakage caused by chitosan was significantly higher from

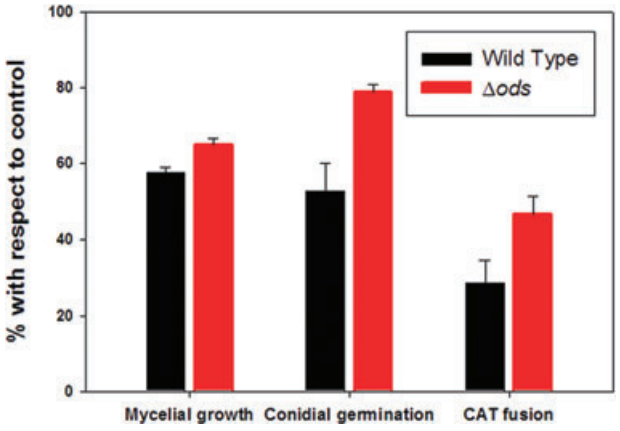

Fig. 3. Resistance to chitosan of a fatty acid desaturase mutant (Δ*ods*) of *N. crassa*. Figure shows chitosan inhibition of mycelial growth (1 mg ml^{-1} chitosan), conidial germination (0.6 µg ml^{-1} chitosan) and CAT fusion (0.6 µg ml^{-1} chitosan). Values are percentage mycelial growth/conidial germination/CAT fusion relative to corresponding control values without chitosan. The mutant was significantly more resistant ($P < 0.05$) for each treatment. Each value (±SE) represents the mean of three replicates.

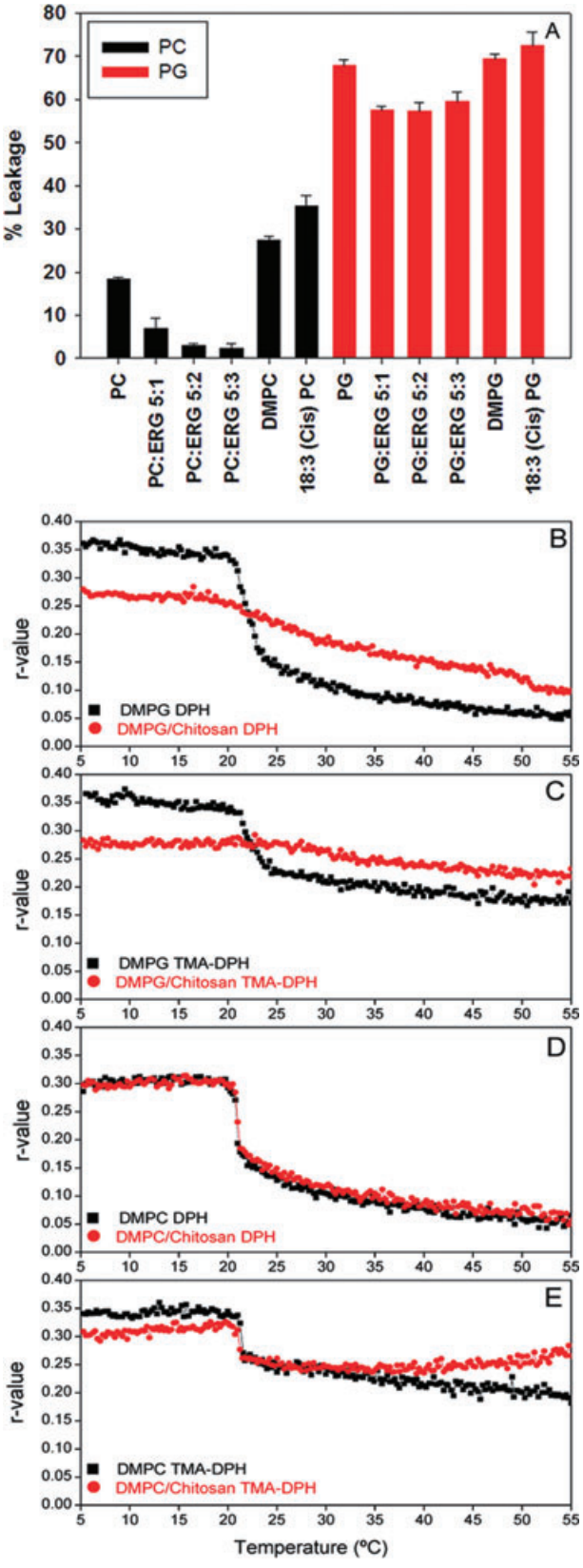

Fig. 4. Effect of chitosan on liposomes of different lipid composition.
A. Percentage leakage (±SE) of calcein dye encapsulated within different liposomes.
B–E. Steady-state fluorescence anisotropy (*r* value) as a function of temperature of DMPC- and DMPG-containing membranes in the absence or presence of chitosan. Chitosan to lipid molar ratio was 15:1 in the four graphs. PC, L-α-phosphatidylcholine; PG, L-α-phosphatidylglycerol; ERG, ergosterol; DMPC, 1,2-dimyristoyl-sn-glycero-3-phosphocholine; 18:3 (Cis) PC, 1,2-dilinolenoyl-sn-glycero-3-phosphocholine; DMPG, 1,2-dimyristoyl-sn-glycero-3-[phospho-rac-(1-glycerol)]; 18:3 (Cis) PG, 1,2-dilinolenoyl-sn-glycero-3-phospho-(1′-rac-glycerol); DPH, 1,6-diphenyl-1,3,5-hexatriene; TMA-DPH, 1-(4-trimethylammoniumphenyl)-6-phenyl-1,3,5-hexatriene.

liposomes composed of membranes with negatively charged phospholipids than from liposomes composed of neutral phospholipids. Unsaturated fatty acids in neutral membranes also increased leakage, which was also consistent with our data indicating that unsaturated fatty acids and increased fluidity of the plasma membrane confer chitosan sensitivity to fungi. Furthermore, the steady-state fluorescence anisotropy experiments suggested that chitosan binds to the membrane surface affecting the cooperativity and anisotropy of the gel and liquid-crystalline phases.

Taken together, our combined data suggest that chitosan first binds to the target membrane surface and covers it in a carpet-like manner as has been reported for other positively charged antimicrobial peptides (Chan *et al.*, 2006). Initial interaction with the negatively charged target membrane is electrostatically driven because of the positive charge of the chitosan. In a second step, after a threshold concentration has been reached, chitosan will cause membrane permeabilization. The effect on the membrane surface will depend on the chitosan concentration and the composition of the target membrane. Our results indicate that the level of fatty acid unsaturation and the extent of membrane fluidity may explain the differences in chitosan sensitivity found in the fungi studied. In a highly polyunsaturated membrane exhibiting high fluidity, chitosan binding should induce an increase in membrane rigidity in the membrane regions to which it attaches. Since negatively charged membrane lipids are not uniformly distributed within the plasma membrane (Alvarez *et al.*, 2007; Jean-francois *et al.*, 2008), this interaction will enhance differences in fluidity between different membrane regions, causing membrane permeabilization. In a saturated, more rigid membrane, the changes in rigidity induced by chitosan binding would be much lower and little permeabilization, even in the presence of negatively charged phospholipids headgroups, should be induced.

It has been previously shown that fatty acid composition is a robust taxonomic tool for classifying fungi below family level (Ruess *et al.*, 2002). The differences in fatty acid profiles observed here are consistent with the resis-

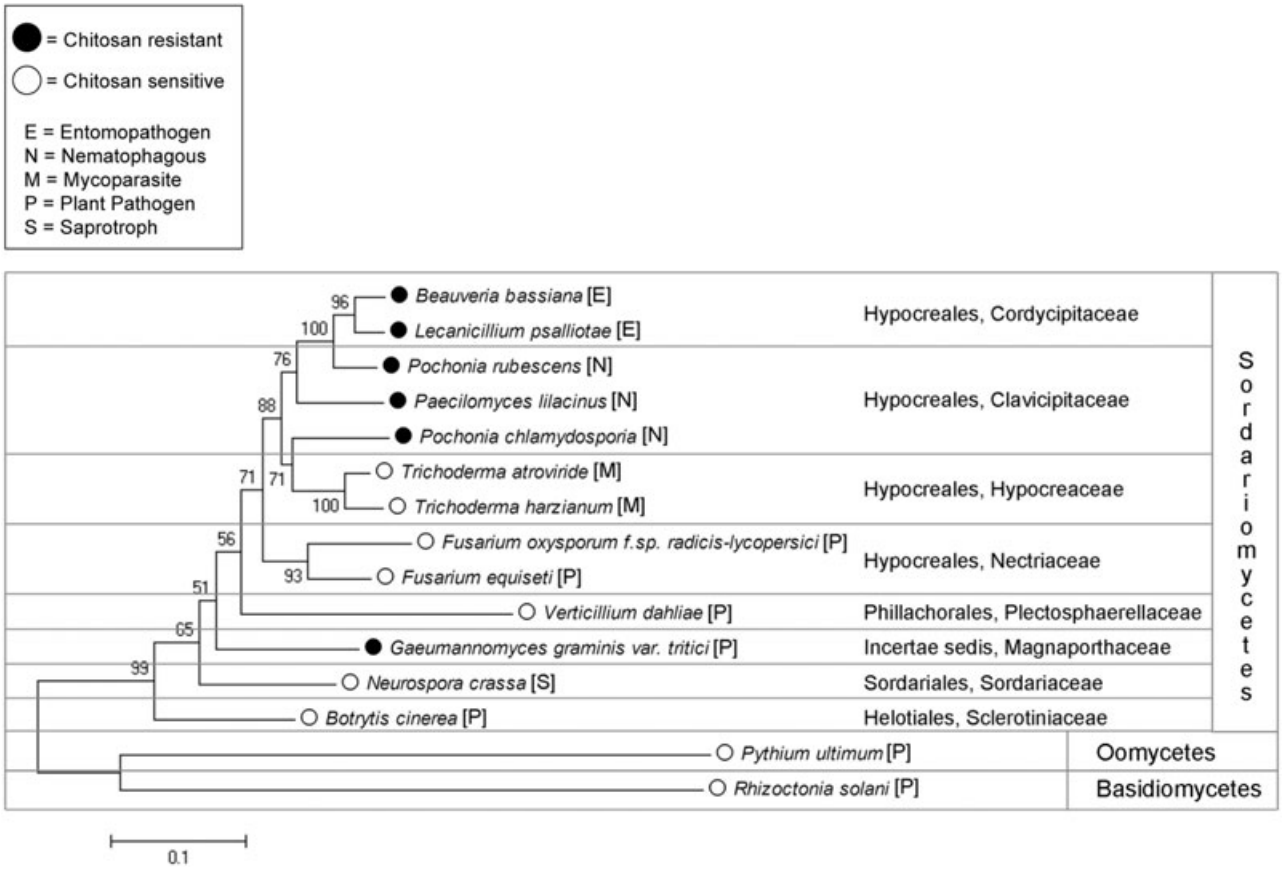

Fig. 5. Phylogenetic analysis of chitosan-sensitive and chitosan-resistant fungi and oomycetes (14,15) based on rDNA ITS sequences from GenBank. Fungi: *Beauveria bassiana* (Accession No. FJ468000), *Lecanicillium psalliotae* (Accession No. AB160994), *Pochonia rubescens* (Accession No. DQ516078), *Paecilomyces lilacinus* (Accession No. EU306174), *Pochonia chlamydosporia* (Accession No. AJ291804), *Trichoderma atroviride* (Accession No. AF278794), *Trichoderma harzianum* (Accession No. FJ442681), *Fusarium oxysporum* f. sp. *radicis-lycopersici* (Accession No. AY354387), *Fusarium equiseti* (Accession No. FJ439592), *Verticillium dahliae* (Accession No. EF015891), *Gaeumannomyces graminis* var. *tritici* (Accession No. AJ969262), *Neurospora crassa* (Accession No. AY681193), *Botrytis cinerea* (Accession No. AB444949), *Rhizoctonia solani* (Accession No. FJ534556). Oomycetes: *Pythium ultimum* (Accession No. EU792322).
(●) = chitosan-resistant fungi; (○) = chitosan-sensitive fungi; E = entomopathogenic fungi; N = nematophagous fungi; M = mycoparasitic fungi; P = plant pathogenic fungi; S = saprotrophic fungi.

tant and sensitive fungi belonging to different fungal families. The chitosan-resistant fungi form a paraphyletic group composed of entomopathogenic fungi (Cordycipitaceae family) and nematophagous egg-parasitic fungi (Clavicipitaceae family) (Fig. 5). Hosts of both groups of fungi have cuticles and egg-shells with a high chitin content (Wharton, 1980; Bird and Bird, 1991) that these fungi have to degrade to penetrate the host (Lopez-Llorca and Duncan, 1988). It has been recently shown that entomopathogenic fungi transform chitin in the host cuticle to chitosan using chitin deacetylases, and this chitosan is later degraded by fungal chitosanases during host penetration (Nahar *et al*., 2004). We previously found that the only chitosan-resistant species that was neither nematophagous nor entomopathogenic, out of 11 species tested, was the root pathogen *Gaeumannomyces graminis* var. *tritici*. However, in contrast to the entomopathogenic and nematophagous fungi, which showed high chitosanolytic activity, *G. graminis* var. *tritici* was unable to degrade chitosan (Palma-Guerrero *et al*., 2008), suggesting that it has evolved a different method of chitosan resistance. We propose that chitosan-resistant entomopathogenic and nematophagous fungi may have evolved to survive the antifungal chitosan residues generated during host penetration by modifying their plasma membrane fluidity to reduce chitosan damage.

Our findings provide important new insights into the mechanism by which chitosan permeablizes fungal plasma membranes, and into the basis of chitosan resistance and its evolution in fungi. Our conclusions also provide a method for predicting the sensitivity of a fungus to chitosan based on its plasma membrane composition. Perhaps most importantly, our results suggest a new strategy for antifungal therapy, which involves treatments that increase plasma membrane fluidity to make fungi more sensitive to fungicides with similar modes of action to

chitosan (e.g. positively charged antimicrobial agents; Jean-francois *et al*., 2008).

Experimental procedures

Strains and culture conditions

Beauveria bassiana, *P. chlamydosporia* and *F. oxysporum f.*sp. *radicis-lycopersici* (strain collection at the Plant Pathology Laboratory, University of Alicante) were maintained on corn meal agar (CMA, Becton Dickinson and Company, Sparks, MD, USA). The *Neurospora crassa* wild-type strain 74-OR23-IVA (FGSC #2489) and the *N. crassa* fatty acid desaturase mutant (FGSC #16054), which we have named Δ*ods*, were maintained on solid Vogel's agar medium (Davis, 2000).

For fatty acid, ergosterol and lipid analyses, fungi were grown on 1% PDB (Potato Dextrose Broth, Becton Dickinson and Company, Sparks, MD, USA) for 5 days, at 25°C with shaking at 100 r.p.m. The resultant mycelium was vacuum-filtered and lyophilized prior to extraction.

Chitosan preparation

Chitosan (T8s) with a molecular weight of 70 kDa and exhibiting 79.6% deacetylation was obtained from Marine BioProducts GmbH (Bremerhaven, Germany). Chitosan was dissolved in 0.25 mol l^{-1} HCl and the pH adjusted to 5.6 with NaOH. The resulting solution was dialysed for salt removal, and the dialysed chitosan was autoclaved at 120°C for 20 min (Palma-Guerrero *et al*., 2008).

Rhodamine-labelled T8s chitosan (R-chitosan) was kindly provided by Dr V. Tikhonov (Laboratory of Physiologically Active Biopolymers, A.N. Nesmeyanov Institute of Organoelement Compounds, Russian Academy of Sciences, Moscow, Russia), and was prepared as described above for T8s chitosan.

Staining of conidia with rhodamine-chitosan

Conidia from the different fungi were collected in sterile distilled water, their concentration was adjusted to 10^6 conidia ml^{-1}, and then they were treated with 0.1 mg ml^{-1} rhodamine-chitosan (final concentration) for 15 min at room temperature. The resultant conidial suspension was then dispensed as 25 μl droplets onto glass coverslips, and conidia were immobilized by the inverted agar block method (Hickey *et al*., 2005) and imaged by confocal microscopy with a 60× oil immersion objective. Confocal laser scanning microscopy was performed using an inverted DM IRBE2 microscope (Leica). Rhodamine-chitosan was imaged using excitation wavelength at 543 nm and fluorescence detection at 555–700 nm. Simultaneous brightfield images were captured with a transmitted light detector. Images were captured with a resolution of 512 × 512 pixels. Confocal images were processed using Image J (version 1.38× for Mac Os) and Adobe Photoshop (version 10.0; Adobe Systems) software.

Fatty acid analysis

After tissue homogenization, the fatty acid composition of the total lipid fraction was determined by fat extraction with a mixture of chloroform and methanol (1:1 and 2:1 proportions for the first and second extractions respectively) following the method of Folch *et al.* (1957). Fatty acid methyl esters (FAME) samples were analysed according to the method of Stoffel *et al.* (1959). Samples were analysed by gas-liquid chromatography using a SPTM 2560 flexible fused silica capillary column (100 m length and 0.25 mm internal diameter and 0.20 μm of film thickness) in a Hewlett-Packard 5890 gas chromatograph (Waldbronn, Germany). The oven temperature was programmed for 5 min at an initial temperature of 140°C, was increased at a rate of 4°C per minute to 230°C, was further increased at a rate of 1°C per minute to 240°C and then was held at this temperature for 6 min. The injector and flame ionization detector were set at 250°C. Helium was used as the carrier gas at a pressure of 290 kPa, and peaks were identified by comparison of their retention times with appropriate FAME standards purchased from Sigma Chemical Company (St Louis, MO, USA). Individual fatty acid concentrations were expressed as percentages of the total content. The fatty acid unsaturation index of each sample was calculated by multiplying the percentage of each fatty acid (relative to the total fatty acids present in the sample) by the number of double bonds it contains and adding the results for all the fatty acids identified in the sample.

Ergosterol analysis

The alkaline ergosterol extraction was performed as described previously (Van leeuwen *et al*., 2008) with some minor modifications. Mycelium (50 mg dry weight) was homogenized in a 15 ml polypropylene screw-cap centrifuge tube containing 4 ml 10% KOH in methanol (Sigma) and an equal amount of 0.5 mm glass beads. The mixture was vortexed for 15 min and sonicated in a bath for another 15 min. The preparation was then heated for 90 min at 70°C in a water bath. For extraction, 1 ml distilled water and 2 ml n-hexane (Sigma) were added at room temperature, vortexed for 30 s, and centrifuged at 3200 *g* for 10 min. The top (n-hexane) fraction was removed and the aqueous fraction was shaken with fresh n-hexane for an additional extraction. The pooled n-hexane fractions were evaporated overnight in a water bath at 45°C. After evaporation the precipitates were dissolved in 1 ml methanol by vortexing and sonication for 10 min. The samples were filtered through an Acrodisc 0.2 μm PTFE syringe filter (Sigma) and loaded for HPLC analysis. Ergosterol was measured using a LiChospher 100 RP-18 (5 μm) column (Agilent Technologies). The mobile phase consisted of methanol at a flow rate of 1.5 ml min^{-1} and ergosterol was detected at 282 nm. The peak area at this wavelength was used for quantification using an external standard (Sigma).

Phospholipid analysis

Phospholipid extraction and analysis were carried out by Mylnefield Lipid Analysis (Dundee, UK). Total lipids were extracted following a method similar to that described for fat extraction prior to fatty acid analysis but with minor modifications (Moilanen and Nikkari, 1981). Two-dimensional thin layer chromatography (TLC) was used to separate the indi-

vidual phospholipids in each fungal sample. TLC plates were run in the first dimension in a mobile phase of 65:22:2.6 chloroform/methanol/water (v/v/v) for 1 h. When developed, the TLC plates were left to dry in an oven at 25°C for 1 h before being turned through 90° and placed back into the developing tank containing a second mobile phase of 80:12:15:4 chloroform/methanol/acetic acid/water (v/v/v/v) for 1 h. When developed, the plates were removed from the tank and incubated at 25°C for 15 min. The plates were then sprayed with 0.01% primulin solution and incubated 25°C for a further 15 min. The plates were viewed under UV light and the individual phospholipid spots were identified and circled with pencil before being scraped off the silica plate into individually labelled test tubes. Toluene (1 ml) and 1% sulphuric acid-methanol solution (2 ml) were added, and the test tubes were then incubated overnight in a heating block at 50°C. After removal from the heating 5% aqueous sodium chloride (5 ml) and iso-hexane (2 ml) were added and the sample was shaken. Once the sample had settled into two layers, the upper iso-hexane layer was drawn off into another test tube with a Pasteur pipette. The original test tube was extracted again with iso-hexane (2 ml), and both iso-hexane fractions (4 ml) were collected in the same test tube. After extraction, 2% aqueous potassium hydrogen carbonate (3 ml) was added to the iso-hexane fractions and the sample was shaken. When settled, the upper iso-hexane fraction was drawn off and passed through a sodium sulphate column, into a centrifuge tube in order to assist the removal of residual water. The centrifuge tube was placed in a centrifugal evaporator to remove the solvent. After the solvent had been removed the remaining oil was re-immersed in a calculated volume of iso-hexane and butylhydroxytoluene, and placed on the gas cromatograph for fatty acid analysis.

Acidic glycosphingolipid analysis

Extraction and analysis of acidic glycosphingolipids were carried out as described previously (Toledo *et al.*, 1999; Bennion *et al.*, 2003; Ferket *et al.*, 2003) with minor modifications. Mycelium (0.5 g dry weight) was homogenized in a 15 ml polypropylene screw-cap centrifuge tube by vortexing for 15 min and sonication in a bath for a further 15 min, once with 10 ml of solvent A (chloroform/methanol 1:1, v/v), and then twice with 10 ml of solvent B (isopropanol/hexane/water 55:25:20, v/v/v). The upper phase was discarded and the sample was once more similarly vortexed and sonicated with 10 ml of solvent A. The four extracts were pooled and dried on a rotary evaporator. The dried residue was partitioned between water and 1-butanol pre-saturated with water (10 ml each) with vigorous shaking in a separatory funnel. The lower (water) layer was removed, and similarly extracted four more times with equal volumes of water-saturated 1-butanol. The five 1-butanol extracts were combined in a round-bottom flask and evaporated to dryness on a rotary evaporator. The dried residue was then treated with 20 ml methanol/water/1-butanol (4:3:1 v/v/v) containing 25–30% methylamine at 55°C for 4 h in a tightly stoppered flask, with occasional shaking. After removal of the reagent solution by rotary evaporation, the residue was resuspended in a minimal volume of solvent C (chloroform/methanol/water 30:60:8, v/v/v) and applied to a column of DEAE-Sephadex A-25 pre-equilibrated with 0.05 M sodium acetate (Ac^- form). Neutral lipids were eluted with five volumes of solvent C. Acidic lipids, including glycosylinositolphosphorylceramides (GIPCs), were eluted with five volumes of 0.5 M sodium acetate in methanol. The acidic fraction was dried by rotary evaporation, resuspended in a minimal volume of methanol, dialysed exhaustively against deionized water, redried by lyophilization, and taken up in solvent B prior to analytical high performance TLC. HPTLC were performed on silica gel 60 plates (Merck, Darmstadt, Germany) using solvent F (chloroform/methanol/water (50:47:14 v/v/v, containing 0.035% w/v $CaCl_2$). Samples were dissolved in solvent B and applied with 10 µl microcaps. Detection was made by spraying TLC plates with Bial's orcinol reagent [orcinol 0.55% (w/v) and H_2SO_4 5.5% (v/v) in ethanol/water 9:1 (v/v)] and heating them briefly to 200–250°C.

Chitosan inhibition of mycelial growth, conidial germination and CAT fusion

Assessment of the inhibitory effects of chitosan on mycelial growth of *N. crassa* wild-type strain and the *Δods* fatty acid desaturase mutant was carried out on PDA plates supplemented with 1 mg ml^{-1} chitosan, as described previously (Palma-Guerrero *et al.*, 2008). PDA plates without chitosan served as controls. Four plates per treatment were inoculated in the centre with a plug (5 mm diameter) from the edge of a 24-h-old colony of the fungus to be tested, and the colony radius was measured after 10 h of growth for each plate. The percentage colony extension in the presence of 1 mg ml^{-1} chitosan relative to the untreated control was calculated. The experiment was performed three times.

For conidial germination and CAT fusion assays conidia were collected from 4- to 5-day-old wild-type or mutant cultures of *N. crassa* by adding 1 ml sterile distilled water and removing the conidial suspension with a pipette. The conidia were counted using a haemocytometer, diluted to the appropriate concentration and immediately used in the bioassays. Conidial germination and CAT fusion assays were carried as described previously (Palma-Guerrero *et al.*, 2009). Conidial germination and CAT fusion assays were carried out in 8-well slide culture chambers (Nalge Nunc International, Rochester, NY). Each well was filled with 200 µl of conidial suspension at a final concentration of 10^6 conidia ml^{-1} in Vogel's medium (Davis, 2000) diluted 100 times. After incubation at 24°C in continuous light, the percentage of conidia that had germinated was quantified (percentage germination was defined as the percentage of conidia possessing one or more germ tubes and/or CATs). A 20× dry or a 60× water immersion plan apo objective with differential interference contrast (DIC) optics on an inverted TE2000E microscope (Nikon, Kingston-Upon-Thames, UK) was used for the analysis of conidial germination. CAT fusion was assessed with the 60× objective on the inverted microscope and CAT fusion was quantified as the percentage of conidia/conidial germlings involved in fusion. Three wells per treatment, with 10 fields of view per well (each containing 100–300 conidia) were assessed, and each experiment was performed twice.

Membrane leakage by chitosan

To study the effect of chitosan on artifical membranes, membrane leakage experiments, based on the release of the fluorescent probe calcein encapsulated in artificial liposomes of different membrane compositions, were performed. L-α-phosphatidylcholine (from chicken egg) (PC), L-α-phosphatidylglycerol (from chicken egg; sodium salt) (PG), 1,2-dimyristoyl-sn-glycero-3-phosphocholine (DMPC), 1,2-dimyristoyl-sn-glycero-3-[phospho-rac-(1-glycerol)] (DMPG), 1,2-dilinolenoyl-sn-glycero-3-phosphocholine (18:3 (Cis) PC), 1,2-dilinolenoyl-sn-glycero-3-phospho-(1′-rac-glycerol) (18:3 (Cis) PG) and ergosterol (ERG) were obtained from Avanti Polar Lipids (Alabaster, AL, USA). Calcein was obtained from Sigma. 1,6-diphenyl-1,3,5-hexatriene (DPH) and 1-(4-trimethylammoniumphenyl)-6-phenyl-1,3,5-hexatriene (TMA-DPH) were obtained from Molecular Probes (Eugene, OR, USA). All other reagents used were of analytical grade from Merck (Darmstadt, Germany). Water was deionized, twice distilled and passed through a Milli-Q equipment (Millipore Iberica, Madrid, Spain) to a resistivity lower than 18 MΩ cm.

Aliquots containing the appropriate amount of lipids in chloroform/methanol (2:1, v/v) were placed in a test tube, the solvents removed by evaporation under a stream of O_2-free nitrogen, and finally, traces of solvents were eliminated under vacuum in the dark for 3 h. The lipid films were resuspended in an appropriate buffer and incubated either at 25°C or 10°C above the gel-to-liquid-crystal-phase transition temperature (T_m) with intermittent vortexing for 30 min to hydrate the samples and obtain multilamellar vesicles (MLV). The samples were frozen and thawed five times to ensure complete homogenization and maximization of chitosan/lipid contacts, with occasional vortexing. Large unilamellar vesicles (LUV) with a mean diameter of 0.1 mm were prepared from MLVs by the extrusion method (Mayer *et al.*, 1986), using polycarbonate filters with a pore size of 0.1 mm (Nuclepore Corp., Cambridge, CA, USA). The phospholipid concentration was measured by methods described previously (Bottcher *et al.*, 1961). For membrane leakage measurements LUVs with a mean diameter of 0.1 mm were prepared as indicated above in a buffer consisting of 20 mM citrate, 20 mM NaCl and 40 mM calcein; pH 5.4 (Perez-berna *et al.*, 2006). Non-encapsulated calcein was separated from the vesicle suspension through a Sephadex G-75 filtration column (Pharmacia, Uppsala, Sweden) and eluted with a buffer containing 20 mM citrate, 100 mM NaCl and 0.1 mM EDTA; pH 5.4. Membrane rupture (leakage) of intraliposomal calcein was assayed by treating the probe-loaded liposomes (final lipid concentration, 0.125 mM) with the appropriate amounts of chitosan using a 5 × 5 mm fluorescence cuvette at a final volume of 400 µl on a Cary Eclipse spectrofluorometer (Varian, San Carlos, CA, USA), stabilized at 25°C. The medium in the cuvettes was continuously stirred to allow for a rapid mixing of chitosan and vesicles. Leakage was assayed until no more change in fluorescence was obtained at excitation and emission wavelengths of 492 and 517 nm respectively. Excitation and emission slits were set at 5 nm. One hundred per cent release was achieved by adding Triton X-100 to the cuvette to a final concentration of 0.5% (v/v). Fluorescence measurements were made initially with probe-loaded liposomes, afterwards by adding chitosan solution, and finally by adding Triton X-100 to obtain 100% leakage. Leakage was quantified on a percentage basis (% L) according to the equation, $\%L = [(F_f - F_o) \times 100]/(F_{100} - F_o)$; where F_f is the equilibrium value of fluorescence after chitosan addition, F_0 is the initial fluorescence of the vesicle suspension, and F_{100} is the fluorescence value after the addition of Triton X-100. Although chitosan induced the release of the internal contents of the liposomes in a dose-dependent manner, we chose a chitosan-to-lipid molar ratio of 15:1 as it was optimal for analysis.

Steady-state fluorescence anisotropy

The effect of chitosan on the structural and temperature-dependent properties of phospholipid membranes was studied using steady-state fluorescence anisotropy. MLVs were formed in 20 mM citrate, 100 mM NaCl and 0.1 mM EDTA, pH 5.4. Aliquots of TMA-DPH or DPH in N,N9-dimethylformamide (2×10^{-4} M) were directly added into the lipid dispersion to obtain a probe/lipid molar ratio of 1:500. Samples were incubated for 15 or 60 min for TMA-DPH and DPH, respectively, at 10°C above the T_m of the phospholipid. Afterwards, chitosan was added to obtain a chitosan/lipid molar ratio of 15:1, and was incubated at 10°C above the T_m of each phospholipid for 1 h, with occasional vortexing. All fluorescence studies were carried using 5 × 5 mm quartz cuvettes in a final volume of 400 µl (315 mM lipid concentration). All data were corrected for background intensities. The steady-state fluorescence anisotropy, $\langle r \rangle$, was measured with an automated polarization accessory using a Varian Cary Eclipse fluorescence spectrometer, coupled to a Peltier device for automatic temperature change. The vertically and horizontally polarized emission intensities, elicited by vertically polarized excitation, were corrected for background scattering by subtracting the corresponding polarized intensities of a phospholipid preparation lacking probes. The G-factor, accounting for differential polarization sensitivity, was determined by measuring the polarized components of the fluorescence of the probe with horizontally polarized excitation ($G = I_{HV}/I_{HH}$). Samples were excited at 360 nm (slit width, 5 nm) and fluorescence emission was recorded at 430 nm (slit width, 5 nm). The values were calculated from the equation by Lakowicz (1999). The steady-state anisotropy was defined by $\langle r \rangle = (I_{vv} - GI_{VH})/(I_{vv} + 2GI_{VH})$; where I_{VV} and I_{VH} are the fluorescence intensities measured (after appropriate background subtraction) with the excitation polarizer vertically oriented and the emission polarizer horizontally oriented.

Phylogenetic analysis

A total of 15 rDNA ITS sequences, containing the internal transcribed spacer 1, the 5.8S ribosomal RNA gene and the internal transcribed spacer 2, were retrieved from GeneBank for fungal species known to be sensitive or resistant to chitosan (Palma-Guerrero *et al.*, 2008; 2009). Sequences were aligned using ClustalX, and were corrected by visual alignment. A neighbour-joining (NJ) tree was produced following the Kimura two-parameter model, using the MEGA program version 4 (Tamura *et al.*, 2007). The tree was resampled 1000 times for bootstrap analysis.

Statistical analyses

Statistical analyses of the data were performed using SPSS 16.0 for Mac OS. To test possible differences between samples we carried out raw data (e.g. fatty acid composition) analyses. To study differences in chitosan sensitivity of mutants (e.g. hyphal growth) we analysed percentages respect to control to normalize the data. One-way ANOVA analysis was used in every case, assuming a *P*-value of 0.05. After that, *post hoc* tests, using the least significant difference method or Tamhane's T2 tests, were used to detect significant differences between treatments.

Acknowledgements

We thank Dr V. Tikhonov for providing the R-chitosan, and Dr J. Martin-Nieto for critical reading of the manuscript. The research was supported by the Spanish Ministry of Science and Innovation (AGL2008-00716) and UK Biotechnological and Biological Science Research Council (BB/E010741/1).

References

Allan, C.R., and Hadwiger, L.A. (1979) The funcidal effect of chitosan on fungi of varying cell wall composition. *Exp Mycol* **3:** 285–287.

Alvarez, F.J., Douglas, L.M., and Konopka, J.B. (2007) Sterol-rich plasma membrane domains in Fungi. *Eukaryot Cell* **6:** 755–763.

Benhamou, N., Lafontaine, P.J., and Nicole, M. (1994) Induction of systemic resistance to *Fusarium* crown and root rot in tomato plants by seed treatment with chitosan. *Phytopathology* **84:** 1432–1444.

Bennion, B., Park, C., Fuller, M., Lindsey, R., Momany, M., Jennemann, R., and Levery, S.B. (2003) Glycosphingolipids of the model fungus *Aspergillus nidulans*: characterization of GIPCs with oligo-alpha-mannose-type glycans. *J Lipid Res* **44:** 2073–2088.

Bird, A.F., and Bird, J. (1991) *The Structure of Nematodes*. San Diego, CA: Academic Press.

Bottcher, C.S.F., Van Gent, C.M., and Fries, C. (1961) A rapid and sensitive sub-micro phosphorus determination. *Anal Chim Acta* **1061:** 203–204.

Chan, D.I., Prenner, E.J., and Vogel, H.J. (2006) Tryptophan- and arginine-rich antimicrobial peptides: structures and mechanisms of action. *Biochim Biophys Acta* **1758:** 1184–1202.

Cohen, E. (1987) Chitin biochemistry: synthesis and inhibition. *Annu Rev Entomol* **32:** 71–92.

Damude, H.G., Zhang, H., Farrall, L., Ripp, K.G., Tomb, J.F., Hollerbach, D., and Yadav, N.S. (2006) Identification of bifunctional delta12/omega3 fatty acid desaturases for improving the ratio of omega3 to omega6 fatty acids in microbes and plants. *Proc Natl Acad Sci USA* **103:** 9446–9451.

Davis, R.H. (2000) *Neurospora: Contributions of a Model Organism*. Oxford: Oxford University Press.

Dodane, V., and Vilivalam, V.D. (1998) Pharmaceutical applications of chitosan. *Pharm Sci Technolo Today* **1:** 246–253.

El Ghaouth, A., and Arul, J. (1992) Antifungal activity of chitosan on post-harvest pathogens: induction of morphological and cytological alterations in *Rhizopus stolonifer*. *Mycol Res* **96:** 769–772.

Ferket, K.K., Levery, S.B., Park, C., Cammue, B.P., and Thevissen, K. (2003) Isolation and characterization of *Neurospora crassa* mutants resistant to antifungal plant defensins. *Fungal Genet Biol* **40:** 176–185.

Folch, J., Lees, M., and Sanley, G.A. (1957) A simple method for the isolation and purification of total lipids from animal tissues. *J Biol Chem* **226:** 497–509.

Hadwiger, L.A., Loschke, D.C., and Teasdale, J.R. (1977) An evaluation of pea histones and disease resistance factors. *Phytopathology* **67:** 755–758.

Helander, I.M., Nurmiaho-Lassila, E.L., Ahvenainen, R., Rhoades, J., and Roller, S. (2001) Chitosan disrupts the barrier properties of the outer membrane of gram-negative bacteria. *Int J Food Microbiol* **71:** 235–244.

Hickey, P.C., Swift, S.R., Roca, M.G., and Read, N.D. (2005) Live-cell imaging of filamentous fungi using vital fluorescent dyes and confocal microscopy. In: *Methods in Microbiology, Vol. 35, Microbial Imaging*. Savidge, T., and Pothoulakis, C. (eds). London: Elsevier, pp. 63–87.

Jean-Francois, F., Castano, S., Desbat, B., Odaert, B., Roux, M., Metz-Boutigue, M.H., and Dufourc, E.J. (2008) Aggregation of cateslytin beta-sheets on negatively charged lipids promotes rigid membrane domains. A new mode of action for antimicrobial peptides? *Biochemistry* **47:** 6394–6402.

Kumar, M.N.V.R. (2000) A review of chitin and chitosan applications. *React Funct Polym* **46:** 1–27.

Laflamme, P., Benhamou, N., Bussieres, G., and Dessureault, M. (1999) Differential effect of chitosan on root rot fungal pathogens in forest nurseries. *Can J Bot* **77:** 1460–1468.

Lakowicz, J. (1999) *Principles of Fluorescence Spectroscopy*. New York: Kluwer-Plenum Press.

Lentz, B.R. (1993) Use of fluorescent probes to monitor molecular order and motions within liposome bilayers. *Chem Phys Lipids* **64:** 99–116.

Liu, H., Du, Y.M., Wang, X.H., and Sun, L.P. (2004) Chitosan kills bacteria through cell membrane damage. *Int J Food Microbiol* **95:** 147–155.

Lopez-Llorca, L.V., and Duncan, G.H. (1988) A study of fungal endoparasitism of the cereal cyst nematode *Heterodera avenae* by scanning electron microscopy. *Can J Microbiol* **34:** 613–619.

Mateo, C.R., Lillo, M.P., Gonzalez-Rodriguez, J., and Acuna, A.U. (1991) Molecular order and fluidity of the plasma membrane of human platelets from time-resolved fluorescence depolarization. *Eur Biophys J* **20:** 41–52.

Mayer, L.D., Hope, M.J., and Cullis, P.R. (1986) Vesicles of variable sizes produced by a rapid extrusion procedure. *Biochim Biophys Acta* **858:** 161–168.

Moilanen, T., and Nikkari, T. (1981) The effect of storage on the fatty acid composition of human serum. *Clin Chim Acta* **114:** 111–116.

Nahar, P., Ghormade, V., and Deshpande, M.V. (2004) The extracellular constitutive production of chitin deacetylase in *Metarhizium anisopliae*: possible edge to entomopathogenic fungi in the biological control of insect pests. *J Invertebr Pathol* **85:** 80–88.

Palma-Guerrero, J., Jansson, H.-B., Salinas, J., and Lopez-Llorca, L.V. (2008) Effect of chitosan on hyphal growth and spore germination of plant pathogenic and biocontrol fungi. *J Appl Microbiol* **104:** 541–553.

Palma-Guerrero, J., Huang, I.C., Jansson, H.-B., Salinas, J., Lopez-Llorca, L.V., and Read, N.D. (2009) Chitosan permeabilizes the plasma membrane and kills cells of *Neurospora crassa* in an energy dependent manner. *Fungal Genet Biol* **46:** 585–594.

Parks, L.W., and Casey, W.M. (1995) Physiological implications of sterol biosynthesis in yeast. *Annu Rev Microbiol* **49:** 95–116.

Patton, J.L., and Lester, R.L. (1991) The phosphoinositol sphingolipids of *Saccharomyces cerevisiae* are highly localized in the plasma membrane. *J Bacteriol* **173:** 3101–3108.

Perez-Berna, A.J., Moreno, M.R., Guillen, J., Bernabeu, A., and Villalain, J. (2006) The membrane-active regions of the hepatitis C virus E1 and E2 envelope glycoproteins. *Biochemistry* **45:** 3755–3768.

Rabea, E.I., Badawy, M.E., Stevens, C.V., Smagghe, G., and Steurbaut, W. (2003) Chitosan as antimicrobial agent: applications and mode of action. *Biomacromolecules* **4:** 1457–1465.

Roca, M.G., Arlt, J., Jeffree, C.E., and Read, N.D. (2005) Cell biology of conidial anastomosis tubes in *Neurospora crassa*. *Eukaryot Cell* **4:** 911–919.

Ruess, L., Häggblom, M.M., García Zapata, E.J., and Dighton, J. (2002) Fatty acids of fungi and nematodes – possible biomarkers in the soil food chain. *Soil Biol Biochem* **34:** 745–756.

Selitrennikoff, C.P. (2001) Antifungal proteins. *Appl Environ Microbiol* **67:** 2883–2894.

Stoffel, W., Chu, F., and Ahrens, E.H.J. (1959) Analysis of long-chain fatty acids by gas-liquid chromatography. Micromethod for preparation of methyl esters. *Anal Chem* **31:** 307–308.

Stössel, P., and Leuba, J.L. (1984) Effect of chitosan, chitin and some aminosugars on growth of various soilborne phytopathogenic fungi. *J Phytopathol* **111:** 82–90.

Tamura, K., Dudley, J., Nei, M., and Kumar, S. (2007) MEGA4: Molecular Evolutionary Genetics Analysis (MEGA) software version 4.0. *Mol Biol Evol* **24:** 1596–1599.

Thompson, P.A., Guo, M., Harrison, P.J., and Whyte, J.N.C. (1992) Effects of variation in temperature on the fatty acid composition of eight species of marine phytoplankton. *J Phycol* **28:** 488–496.

Toledo, M.S., Levery, S.B., Straus, A.H., Suzuki, E., Momany, M., Glushka, J., *et al.* (1999) Characterization of sphingolipids from mycopathogens: factors correlating with expression of 2-hydroxy fatty acyl (E)-Delta 3-unsaturation in cerebrosides of Paracoccidioides brasiliensis and *Aspergillus fumigatus*. *Biochemistry* **38:** 7294–7306.

Trotel-Aziz, P., Couderchet, M., Vernet, G., and Aziz, A. (2006) Chitosan stimulates defense reactions in grapevine leaves and inhibits development of *Botrytis cinerea*. *Eur J Plant Pathol* **114:** 405–413.

Van Leeuwen, M.R., Smant, W., de Boer, W., and Dijksterhuis, J. (2008) Filipin is a reliable *in situ* marker of ergosterol in the plasma membrane of germinating conidia (spores) of *Penicillium discolor* and stains intensively at the site of germ tube formation. *J Microbiol Methods* **74:** 64–73.

Vokt, J.P., and Brody, S. (1985) The kinetics of changes in the fatty acid composition of *Neurospora crassa* lipids after a temperature increase. *Biochim Biophys Acta* **835:** 176–182.

Wharton, D.A. (1980) Nematode egg-shells. *Parasitology* **81:** 447–463.

Zakrzewska, A., Boorsma, A., Brul, S., Hellingwerf, K.J., and Klis, F.M. (2005) Transcriptional response of *Saccharomyces cerevisiae* to the plasma membrane-perturbing compound chitosan. *Eukaryot Cell* **4:** 703–715.

Zakrzewska, A., Boorsma, A., Delneri, D., Brul, S., Oliver, S.G., and Klis, F.M. (2007) Cellular processes and pathways that protect *Sacharomyces cerevisiae* against the plasma membrane-perturbing compound chitosan. *Eukaryot Cell* **6:** 600–608.